Needle Tumor Puncture Detection Using a Force and Position Sensor

Joey Greer and Nathan Usevitch

(Dated: 11 December 2015)

Preforming a tumor ablation procedure involves precisely positioning an ablation probe in a tumor. Limited sensing accuracy and variations in tissue properties require that surgeons often identify when they have correctly positioned the probe through their sense of touch. In this paper, supervised learning is used to detect the point at which a needle has entered a tumor using a combination of force and position data. A classifier is developed that uses force data to detect a puncture event, and a Bayesian network that incorporates a position estimate to distinguish between puncture events that may occur because of tissue variations, and puncture events that indicate the target has been reached.

I. INTRODUCTION

Tumor ablation is a minimally invasive technique to treat cancer. It involves guiding the tip of an electric probe to the tumor to be treated and running a current through the probe once the tip of the probe has been positioned in the tumor. The electric current destroys the cancerous tissue through heat. Often times it is difficult for the clinician to know that he or she has successfully reached the tumor, even with the aid of intraoperative imaging such as ultrasound or computed tomography (CT). When this happens, the clinician falls back on his or her sense of touch to know that they have successfully reached their target, since often times the tumor is stiffer than the surrounding, non-cancerous tissue. This project applies machine learning to the problem of detecting when the ablation probe has successfully been placed inside a tumor, using a combination of position data obtained from imaging, as well as force data gathered from an instrumented needle. Enabling an instrumented needle to autonomously detect tumor penetration would enable robotically steered needles to be used in procedures where puncture detection had previously necessitated a human operator. In addition, this classifier could be used as a tool by physicians to more confidently identify when they have reached a tumor. Ideally, the classifier making this prediction would be able to classify tumors in materials of a variety of properties, as material properties of human tissue can vary between people and based on location in the body.

II. PRIOR WORK

Analyzing the forces of needle insertion has been a topic of interest in the medical robotics community for around a decade. Previous work has focused on mechanics modeling and prediction[5,7], which analyze the forces of needle insertion in terms of tissue friction, tissue stiffness, and transient events such as membrane puncture, which is of particular interest in this work. Recently, Elayaperumal *et al.*[1] designed a custom needle sensor to measure forces at the needle tip and play these forces back via haptic actuators to the clinician. Finally, Gonenc *et al.*[2] recently used a custom force sensor to detect vein puncture for retinal surgery in the eye, but relied on heuristic to perform the detection, rather than machine learning techniques.

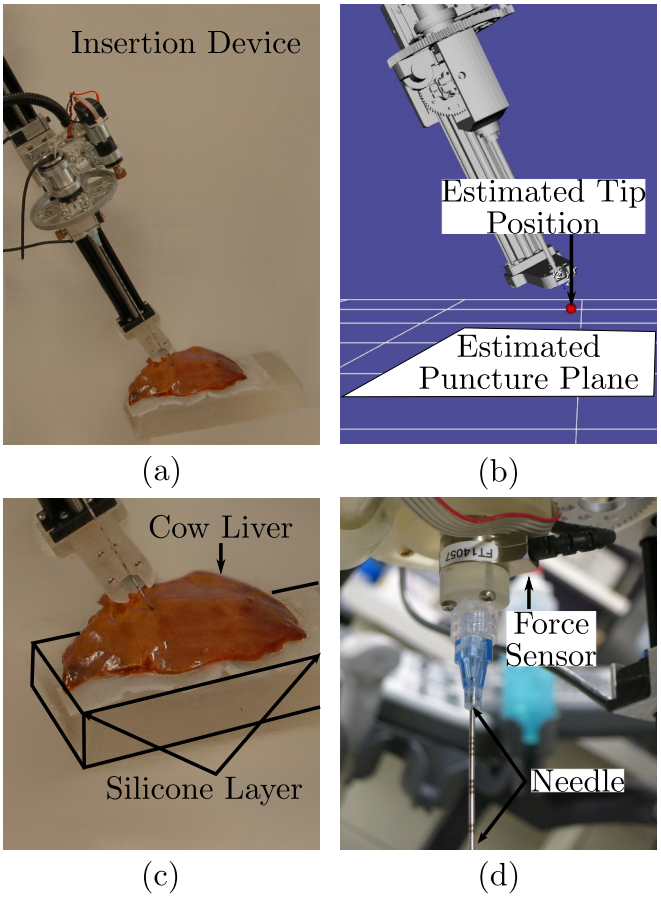

FIG. 1. Expeirmental setup. The needle steering device, (a) is used to insert the needle, shown in (d), at a constant insertion velocity. Two tissue phantoms were used: a cow liver on top of a layer of EcoFlex 00-30 silicone rubber (simulating cancerous tissue), shown in (c), and a block of Polyvinyl Chloride on top of silicone rubber, which was used for collection of training data. (d) Shows a zoomed in picture of the ATI Industrial Automation Nano 17 Force Sensor attached to the base of the needle used for data collection in this paper.)

In this work, we are using time series data as one input modality for classification. Times series offer a unique set of challenges for classification and several approaches exist to using this data, which is covered well in a survey by Keogh *et al.*[3]. Popular methods include using Hidden Markov Models for time series segmentation, where the latent variables correspond to segment labels[4] and time series transforms such as the Discrete Fourier Transform

and various forms of the Wavelet Transform to reduce the dimensionality of the time series for classification. In this work, we use a sliding window approach, where a window of force values, centered around the point in time to be classified are transformed by a featurization function $\phi(\cdots)$ (section III) and used for classification. This method was chosen due to it simplicity and effectiveness on our data.

III. EXPERIMENTAL SETUP AND DATA

Data was collected using a custom needle insertion device (Figure 1(a)) with an insertion stage powered by a DC motor. A straight needle, used to simulate an ablation probe, was mounted on the insertion stage and an ATI Industrial Automation Nano 17 force sensor (Figure 1(d)) and Asenscion technologies electromagnetic tracker were mounted at the base of the needle. Two data modalities were collected over the course of an insertion: axial force magnitude, $f(t)$ and estimated distance between target and needle, $d(t)$. The goal of this work is to develop an algorithm that can detect puncture events in near real-time using force and distance data by estimating

$$P\left(\rho(t) = 1 \mid \phi\left(\vec{f}(t-W), \ldots, \vec{f}(t+W)\right), d(t)\right)$$

using supervised learning. $\rho(t) = 1$ corresponds to the event that a puncture occurred at time t, and $\rho(t) = 0$ corresponds to no puncture at time t. $\phi : \mathbb{R}^{2W+1} \rightarrow \mathbb{R}^n$ corresponds to a featurization of a window of force data (section IV).

Two types of tissue phantoms were used. The first was for testing purposes and consisted of a cow liver, on top of a silicone membrane, which was resting on a slab of gelatin (Figure 1(c)). The silicone membrane and slab of gelatin were used to simulate a tumor to be punctured. Another tissue phantom was used for training data collection, and consisted of a slab of homogeneous gelatin tissue on top of a silicone membrane, which was on top of another slab of gelatin tissue of different stiffness. Again, the silicone membrane and second slab of gelatin tissue were used to simulate a tumor to be punctured. The second tissue phantom was used to collect training data due to its greater re-usability, which allowed for more data collection.

Before each test, the needle steering apparatus was re-oriented to provide a different insertion angle and controlled to insert the needle into the tumor phantom at a constant velocity between 2 mm/s and 6 mm/s. The training set used in this project contains 100 different puncture events in which angle of insertion as well as insertion velocity were varied between tests. A typical force-distance time series collected from a single insertion through the liver and into a silicone membrane is shown in figure 2.

IV. FORCE TIME SERIES CLASSIFICATION

From each time series collected in these experiments several windows of force data were extracted to form a training data set. The windows centered on the puncture along with N other random intervals were selected as training data for the classifier. Parameters to consider when designing the force classifier were feature type, classifier type, training data weighting (to address class imbalance), and window size. To guide these decisions, 10-fold cross validation was used.

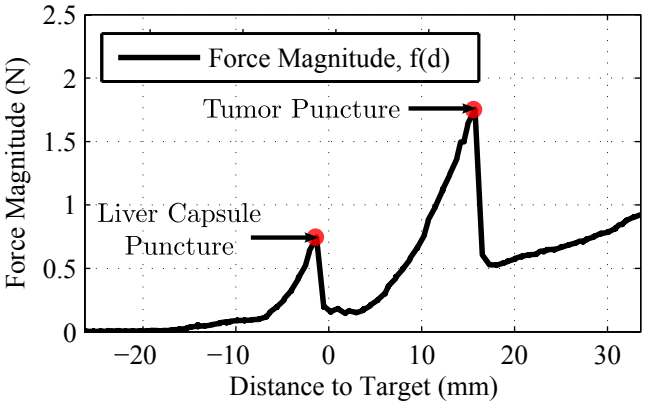

FIG. 2. A typical force and position time series collected from a single insertion through the cow liver and silicone layer. A first puncture type event occurs when the needle punctured the liver capsule. The tumor puncture occurs at a distance past the estimated distance to target because the membrane deflects before the needle punctures through the membrane.

Several parameters were analyzed to design the force classifier. Two types of features were considered for a particular window of force values: raw force values that were normalized (so as to make the classifier able to generalize) and combinations of different slope values (first half slope, second half slope, first quarter slope, last quarter slope). In addition two types of classifiers were considered: logistic regression and regularized logistic regression (a lasso penalty was used and the penalty parameter, λ, was chosen using cross validation.) (Note that Support Vector machines were not considered because we needed a probability of puncture output for the purposes of the combined classifier explained in section V.) Finally, the effect of adding in quadratic combinations of features were considered. The results of different combinations of these options are shown in figure IV, with specificity and sensitivity as the error metrics in order manage effects of class imbalance. The best results were obtained using raw (normalized) force values combined with quadratic combinations of these values, and a regularized logistic regression classifier. Once these parameters were chosen, we considered the effect of window size for force data. Again, 10-Fold cross validation was used to guide our decision process (figure 4). Based on this experiment, a window size of 7 time steps was selected.

V. POSITION DATA

Intuitively, we expect $d(t)$, the estimated distance between the needle tip and target to be near zero when puncture occurs. Due to position noise, elasticity in the target, and mechanical movement, $d(t)$ is not a reli-

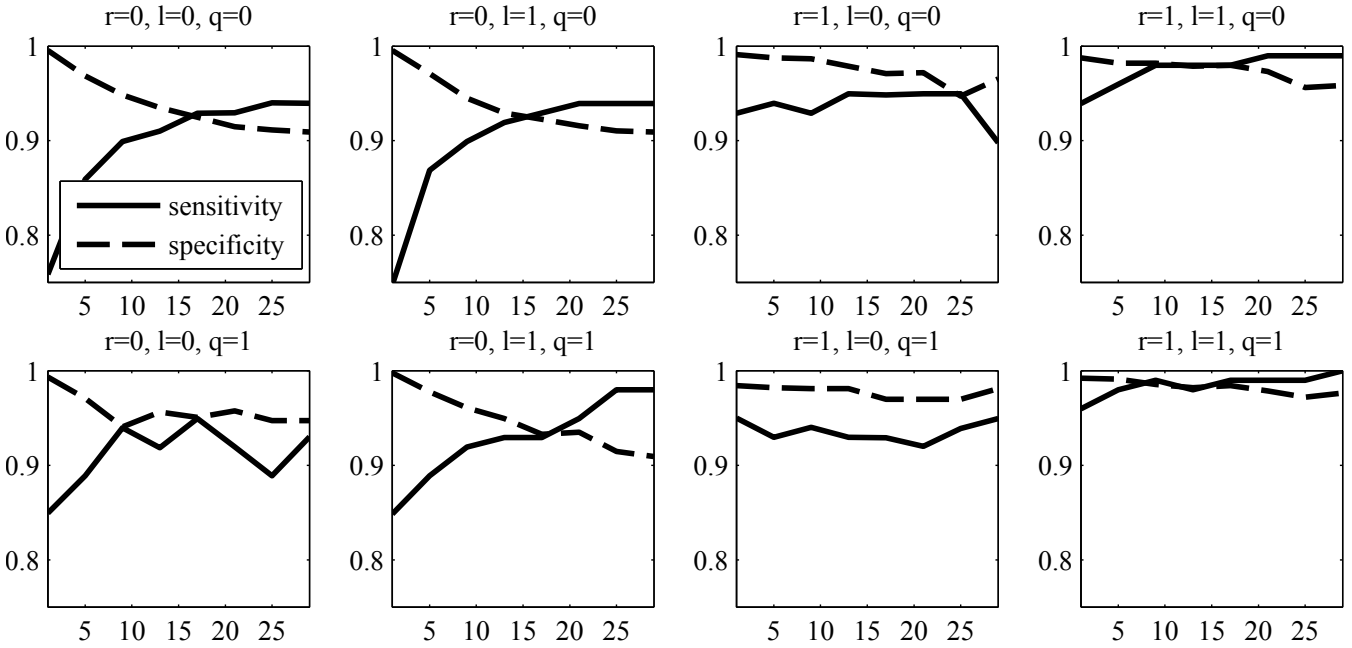

FIG. 3. In this plot, the effect of different combinations of features and classifiers were considered on classifier performance using 10-Fold cross validation on our data. Each plot contains a label $r = a, l = b, q = c$ where $a, b, c \in \{0, 1\}$. $r = 0$ corresponds to using slope ratio features and $r = 1$ corresponds to raw force values on a window centered around the point to be classified. $l = 0, 1$ correspond to using non-regularized and regularized logistic regression, respectively. Finally, $q = 0, 1$ correspond to adding quadratic combinations of features (either slope ratios or raw force values depending on the value of r), respectively. The x-axis of these plots correspond to the weighting used on positive examples to address class imbalance (*i.e.* an x-axis value of 5 corresponds to positive examples being weighted by 5 times over negative examples in the classifier objective function.) Based on these plots, raw force values were used, with regularized logistic regression and quadratic features.

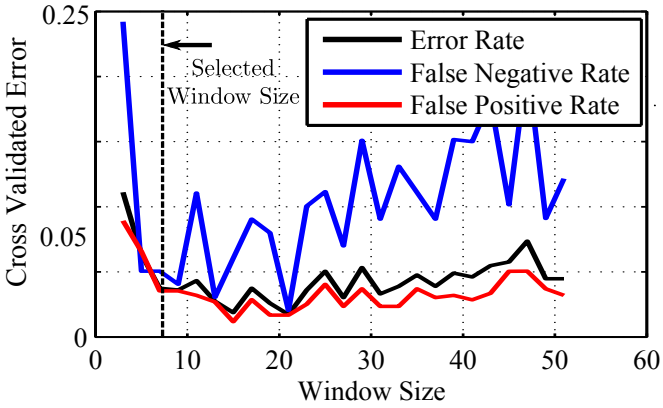

FIG. 4. The effect of changing window size on performance of logistic regression classifier using raw force features. Error rates are obtained by 10 fold cross validation. A window size of 7 is selected.

able indicator by itself, however it is useful for classification. There are two ways to include this data for classification. The simplest way is to include $d(t)$ alongside $\phi\left(\vec{f}(t-W),\ldots,\vec{f}(t+W)\right)$ and train a discriminative classifier to model

$$P\left(\rho \mid \phi\left(\vec{f}(t-W),\ldots,\vec{f}(t+W)\right), d(t)\right)$$

directly. However, as stated before, we know more about the relationship between $d(t)$ and $\rho(t)$. Namely, we expect $d(t)$ to be near zero when puncture occurs. Therefore, we seek to encode this relationship between $d(t)$ into our classifier. To do this, we model the conditional structure of the random variables $\rho(t), \phi\left(\vec{f}(t-W),\ldots,\vec{f}(t+W)\right), d(t)$ as a Bayesian network (figure 6). Assuming the structure between puncture, force, and distance given by the Bayesian network, we can write the joint probability of these variables as

$$P\Big(\rho(t)=1, \phi(\cdots), d(t)\Big) = P\Big(d(t) \mid \rho(t)=1\Big) P\Big(\rho(t)=1 \mid \phi(\cdots)\Big)$$

Given, that we are interested in the quantity $P\left(\rho(t) \mid \phi\left(\vec{f}(t-W),\ldots,\vec{f}(t+W)\right), d(t)\right)$, we would like to compute this quantity in terms of the two conditional distributions we are training, $P(d(t) \mid \rho(t))$ and $P\left(\rho(t) \mid \phi\left(\vec{f}(t-W),\ldots,\vec{f}(t+W)\right)\right)$. Using Bayes Rule and the conditional independence assumptions of the Bayesian network structure in figure 6 we arrive at the following formula

$$P\Big(\rho(t) \mid d(t), \phi(\cdots)\Big) = \frac{P\Big(d(t) \mid \rho(t)\Big) P\Big(\rho \mid \phi(\cdots)\Big)}{\sum_{\rho(t)\in\{0,1\}} P\Big(d(t) \mid \rho(t)\Big) P\Big(\rho(t) \mid \phi(\cdots)\Big)} \tag{1}$$

The log likelihood of the joint probability of puncture, distance, and force takes the following form, which is the

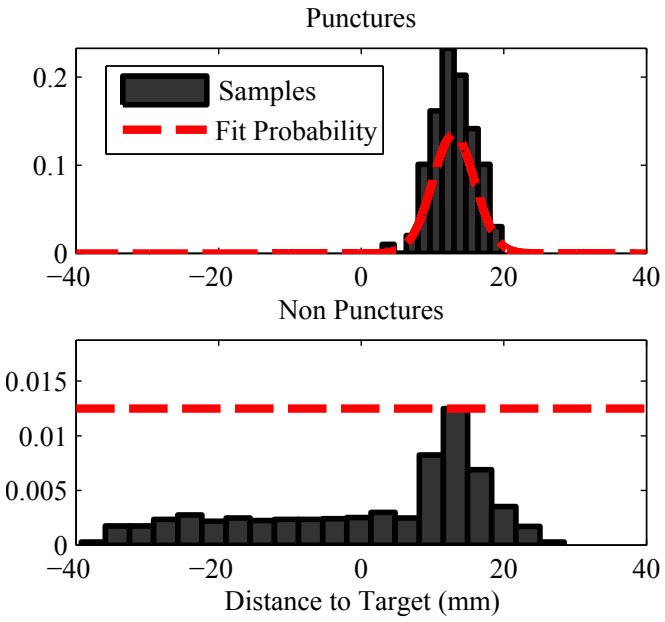

FIG. 5. Experimentally obtained probability distributions of distance given puncture, and distance given no puncture. A Gaussian distribution was fit to the distribution of distance given puncture, and a uniform distribution was used to approximate the distance to the target if there was no puncture. Note that the mean of the probability given puncture is past zero because of the elasticity of the membrane.

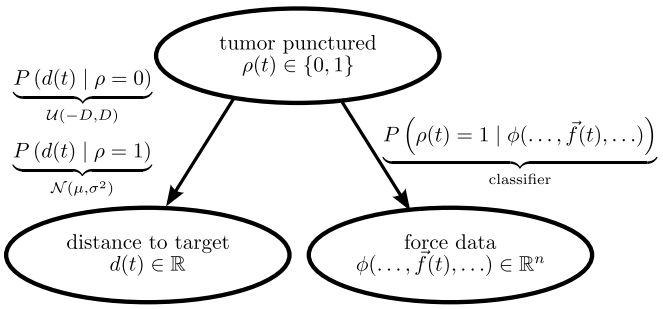

FIG. 6. Bayesian network structure governing the joint probability of $\left(\rho(t), d(t), \phi\left(\vec{f}(t-W),\ldots,\vec{f}(t+W)\right)\right)$. $p\left(\rho(t) \mid \phi\left(\vec{f}(t-W),\ldots,\vec{f}(t+W)\right)\right)$ is calculated using a discriminative classifier such as logistic regression. $P\left(d(t) \mid \rho(t)=1\right)$ is modeled as a normal distribution with mean μ and variance σ^2. This encodes our knowledge and uncertainty about the relationship between puncture and distance.

sum over training examples $1,\ldots,M$

$$l(\theta,\mu,\sigma) = \sum_{i=1}^{M} \log\left(P\left(\rho^{(i)}, d^{(i)}, \phi^{(i)}; \mu,\sigma,\theta\right)\right) =$$

$$\sum_{i=1}^{M} \log\left(P\left(\rho^{(i)}, d^{(i)}, \phi^{(i)}; \mu,\sigma,\theta\right)\right) =$$

$$\sum_{i=1}^{M} \underbrace{\log\left(P\left(d^{(i)} \mid \rho^{(i)}; \mu,\sigma\right)\right)}_{\text{only depends on } \mu,\sigma} + \sum_{i=1}^{M} \underbrace{\log\left(P\left(\rho^{(i)} \mid \phi^{(i)}; \theta\right)\right)}_{\text{only depends on } \theta}$$

where θ are the parameters that govern the classifier $P\left(\rho(t) \mid \phi\left(\vec{f}(t-W),\ldots,\vec{f}(t+W)\right)\right)$. This shows that in order to fit parameters $\hat{\theta}, \hat{\mu}, \hat{\sigma}$ that maximize the joint likelihood of our data, we can separately train the force classifier and Gaussian parameters. The force classifier was discussed in section IV and the maximum likelihood mean and standard deviation governing the distance distribution are found to correspond to the sample mean and variance of distances corresponding to puncture events in the training data set, as shown in figure 5 and given by:

$$(\hat{\mu},\hat{\sigma}) = \underset{\mu,\sigma}{\operatorname{argmax}}\, l(\theta,\mu,\sigma)$$

$$M^{\text{pos}} = \sum_{i=1}^{M} 1\{y^{(i)} = 1\}$$

$$\hat{\mu} = \frac{\sum_{i=1}^{M} 1\{y^{(i)} = 1\} d^{(i)}}{M^{\text{pos}}}$$

$$\hat{\sigma}^2 = \frac{\sum_{i=1}^{M} 1\{y^{(i)} = 1\}(d^{(i)} - \hat{\mu})^2}{M^{\text{pos}}}$$

Finally, to make a prediction using this Bayesian network structure, and optimized parameters, equation 1 is used.

Note that, in this work, we chose to maximize the joint probability, $P(\rho(t), \phi(\cdots), d(t))$, due to the simplistic objective function decomposition that allows us to separately maximize the force and distance probability distributions. Another option is to directly maximize the conditional probability we are interested in, $P(\rho(t) \mid \phi(\cdots), d(t))$. This trade off is discussed in further detail by Roos *et al.*[6] in the general context of Bayesian networks.

VI. PERFORMANCE OF COMBINED CLASSIFIER

To qualitatively test the performance of the force classifier on the measured data, both the classifier that uses force only, and the classifier that incorporates force and distance were used on the liver data. For this test, a moving window was run across all of the data, with the probability of puncture being calculated for each point. Figure 7 shows the time series along with the probability of puncture as computed by the force only classifier and force/position classifier. The force only classifier is accurate at classifying nearly all peaks as puncture events, even the peaks that occur before the actual puncture. The use of the classifier that includes the position estimate prevents peaks away from the puncture from being classified as the puncture event. The position data enabled the algorithm to discriminate between a generic puncture event, and a puncture event that signals when the needle has reached the target region.

VII. CONCLUSION

A regularized logistic regression classifier is developed to detect a puncture event using normalized values from the force time series as features. Despite using training data obtained from a gelatin phantom, the classifier was

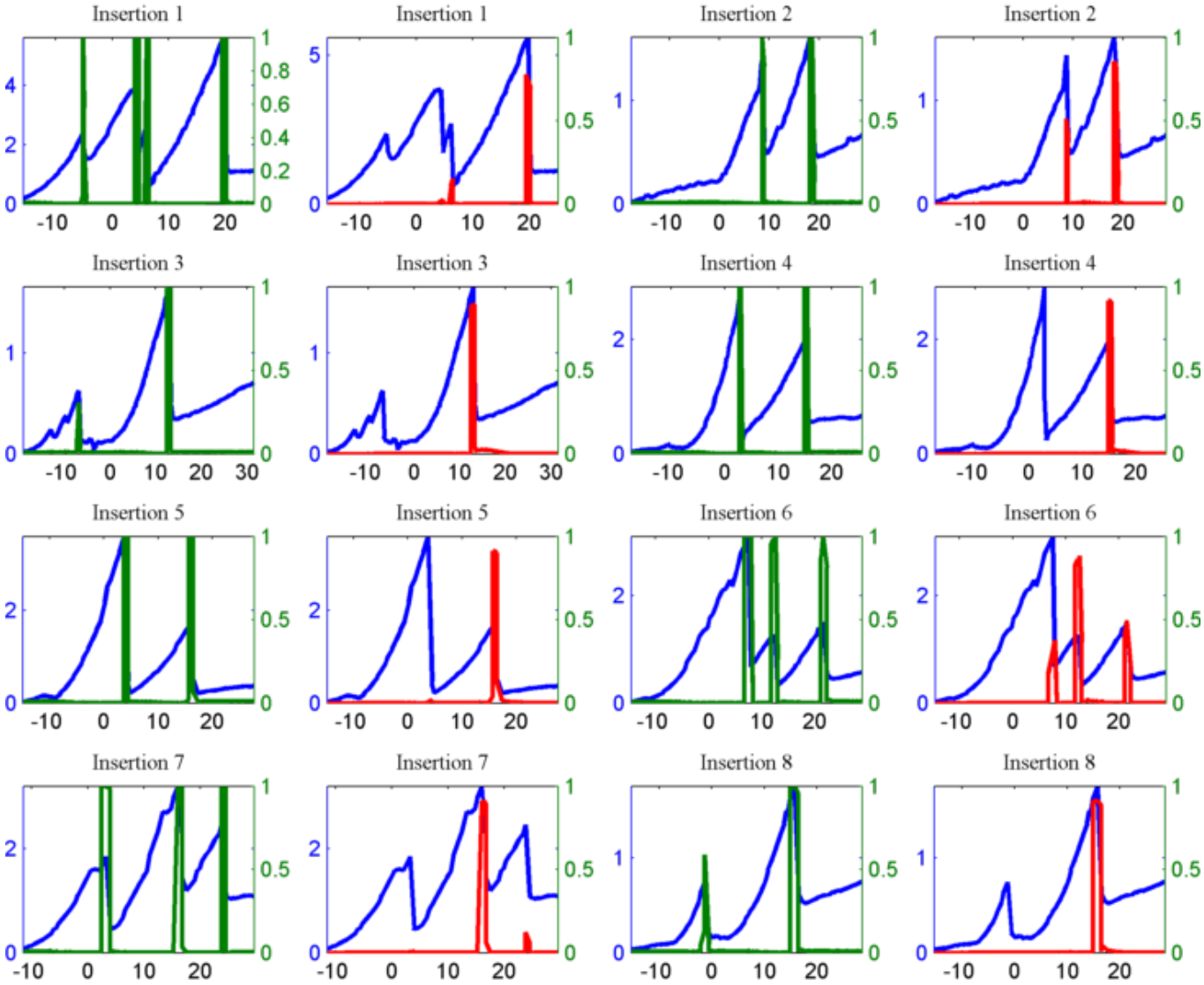

FIG. 7. Results of classification on liver data when using only the force classifier (green), and when using the combined force and position classifier (red). The combined classifier is able to prune false positives based on position.

able to detect puncture-type events during testing in cow liver. Inclusion of data giving a position estimate through a Bayesian network allowed the classifier to distinguish between puncture type events that occurred as the needle passed through liver tissue, and the puncture of the target. This Bayesian network proved an effective way to combine two different modalities of data. This classifier could give physicians an extra tool in identifying when a needle has reached a target during an operation such as a tumor ablation procedure. In addition, this classifier could enable robotically steered needles to perform procedures in which some sort of force information is needed to identify when a target area has been reached, which previously was only possible with a human surgeon.

VIII. BIBLIOGRAPHY

[1]S. Elayaperumal, J. H. Bae, B. Daniel, and M. Cutkosky. Detection of membrane puncture with haptic feedback using a tip-force sensing needle. In *Intelligent Robots and Systems (IROS 2014), 2014 IEEE/RSJ International Conference on*, Sept 2014.

[2]B. Gonenc, S. Member, N. Tran, C. N. Riviere, S. Member, P. Gehlbach, R. H. Taylor, I. Iordachita, and S. Member. Force-Based Puncture Detection and Active Position Holding for Assisted Retinal Vein Cannulation *. 2015.

[3]E. Keogh and S. Chu. Segmenting Time Series : A Survey and Novel Approach.

[4]S. Kim. Segmental Hidden Markov Models with Random Effects for Waveform Modeling. 1:1–27, 2000.

[5]A. M. Okamura, C. Simone, and M. D. O'Leary. Force modeling for needle insertion into soft tissue. *IEEE transactions on bio-medical engineering*, 51, 2004. ISSN 0018-9294. doi: 10.1109/TBME.2004.831542.

[6]T. Roos, H. Wettig, P. Grnwald, P. Myllymki, and H. Tirri. On discriminative bayesian network classifiers and logistic regression. *Machine Learning*, 59(3):267–296, 2005.

[7]T. Washio and K. Chinzei. Needle force sensor, robust and sensitive detection of the instant of needle puncture. 3217, 2004. doi:10.1007/978-3-540-30136-3˙15.